ANALYSIS AND MODELLING OF FRAGMENTS A/M DISTRIBUTIONS FROM IN-ORBIT COLLISIONS

Lorenzo Olivieri[(1)], Alessandro Francesconi[(2)]

[(1)] DII/CISAS, University of Padova, Via Venezia 1, 35131 Padova PD, Italy, Email: lorenzo.olivieri@unipd.it
[(2)] DII/CISAS, University of Padova, Via Venezia 1, 35131 Padova PD, Italy, Email: alessandro.francesconi@unipd.it

ABSTRACT

Area-to-mass data from in-space fragmentation events are currently obtained from space debris observations. The characterization of these objects is limited by the observation systems resolution: frequently, the small-size population cannot be directly observed and reconstructed. Additional information can be collected from ground experiments; however, hypervelocity tests usually employ small targets (below 100 kg) and the achievable EMRs are often below 100 g/J, while historical in-orbit events involved larger bodies and had orders of magnitude higher EMRs. Therefore, existing analytical break-up models, such as the NASA SBM, may have been developed on limited dataset; in addition, the introduction of novel materials and design solutions in modern spacecraft may affect the reliability of these models.

In this context, it has been observed that the A/m distributions are influenced by debris size; in this work it is proposed to divide them in three different regimes based on different break-up mechanisms affecting the fragmentation process. Furthermore, it is noted that the distributions from observations are mostly limited to fragments belonging only to the intermediate size class, whereas the largest class is statistically negligible in the current representation of A/m histograms; on the contrary, ground experiments often include a larger number of objects from the smallest class. A more effective representation is therefore proposed, in terms of cumulative distributions divided per size classes, to better represent the significance of each class.

1 INTRODUCTION

In-orbit collisions can generate thousands of fragments [1], which may cause concerns for the safety of space assets [2]. The risk of fragmentation and orbit pollution is further aggravated [3] by the continuous growth of orbital launches [4] and the deployment of large constellations of thousands of spacecraft [5]. To characterize a debris cloud from an in-space fragmentation, it is essential to know the fragment size, velocity, and area-to-mass ratio (A/m) [6]; in particular, the last parameter is fundamental to evaluate the effect of perturbations (atmospheric drag and solar pressure) in long-term orbital propagations [7][8].

Data on collision events is mostly collected with ground observations and processed to obtain the A/m [9][10]; for the largest in-orbit break-ups, distributions of this parameter can be found in literature [11]. Additional information on the A/m can be collected from ground experiments; however, hypervelocity tests usually employ small targets (below 100 kg) and the achievable EMRs are often below 100 g/J [12][13][14][15], while historical in-orbit events involved larger bodies and had orders of magnitude higher EMRs [16]. Furthermore, the characterization of in-space fragmentations is limited by the ground observation systems resolution [17]: the small-size population cannot be directly observed and reconstructed. A potential issue with experimental and observation A/m data is also related to the fraction of objects belonging to different population classes. In fact, despite their inherent danger for the environment, a few tens of large objects with a particular average A/m ratio may appear statistically insignificant and unnoticeable when compared to hundreds of smaller objects with different A/m ratio values. This represents a significant limitation for the analysis of A/m distributions, which are typically represented as histograms, as they can be distorted by the specific population under consideration.

To date, the most employed analytic break-up model, the NASA SBM, represents the A/m as a sum of normal distributions, whose parameters depend on the fragments size [6]. This approach allows considering different regimes for the A/m trends, with large, medium, and small-size fragments generating different distributions. However, the introduction of novel materials and design solutions in modern spacecraft are currently affecting the reliability of this model, which may require a future update [18][19]. For example, for a set of simplified ground experiments[13] [20], Hanada proposed an improved model based on low-density and high-density materials [21], showing that the A/m distributions trend can be related to the presence of multiple materials.

The presence in the A/m distributions of a dependence from size for the different regimes has been also reported from experimental data (e.g. from SOCIT data [22]). It can be therefore expected that the different regimes might be related to different break-up mechanisms involved in the fragmentation process. In fact, it has been observed from simulations and experiments that the collisional break-up could be represented as the sum of

Proc. 9th European Conference on Space Debris, Bonn, Germany, 1–4 April 2025, published by the ESA Space Debris Office
Editors: S. Lemmens, T. Flohrer & F. Schmitz, (http://conference.sdo.esoc.esa.int, April 2025)

three different mechanisms: the separation of entire parts not directly involved in the fragmentation, the detachment of large components or subsystems due to the failure of structural links, and the fine fragmentation of the parts directly hit [23]. While these mechanisms are recognized to influence the fragments size distribution [24], a similar response can be also expected for the A/m ratios, with three different populations directly recognizable: large parts, intermediate objects, and small debris, each one with different A/m distributions. Furthermore, it can be expected that distribution data from observations are predominantly limited to fragments belonging only to the intermediate class, generally above 10 cm in size, while the largest class is statistically negligible in the current representation of A/m histograms. In contrast, ground experiments often include a larger number of objects from the smallest class, which may reduce the statistical significance of intermediate and large class fragments.

On these considerations, the need of a novel approach in formulating and visualizing the A/m distributions is clear. While preserving a simple formulation is important for the implementation of distributions in numerical models, the reliability of the A/m equations shall be improved. In addition, it is of paramount importance to distinguish among the different breakup mechanisms and size classes in order to individually evaluate each population without compromising statistical significance. The information on a few large debris items might be as important as the distribution of hundreds of small fragments. In the remainder of this paper, an overview of the current models for A/m is presented, with a detailed analysis of their fields of application and potential limitations. In particular, the application of the NASA SBM to various observational and experimental data is explored. A discussion on the common features of A/m distribution models follows, along with a proposal to better represent individual populations in terms of cumulative distributions. Finally, the preliminary steps in the development of an updated A/m distribution model are presented.

2 CURRENT A/M MODELS AND THEIR LIMITATIONS

To date, the most employed model for space debris A/m distributions is part of the NASA SBM [6]; it is used in most fragmentation software and analyses available in literature. The distributions were derived by analysing the decay rates of thousands of debris catalogued by the Space Surveillance Network and from ground-based experiments. For fragments with a characteristic length L_c greater than 11 cm, the A/m distributions were obtained by studying the orbital decay of catalogued debris. The model is then represented by the sum of two normal distributions (in logarithmic space, $\log_{10} A/M$), weighted by a coefficient α; mean, standard deviation, and α are all functions of the logarithm of the characteristic length $\lambda_c = \log_{10} L_C$.

$$D(\log_{10} A/M) = \alpha \cdot N(\mu_1, \sigma_1) + (1-\alpha) \cdot N(\mu_2, \sigma_2) \quad (1)$$

For objects with L_c less than 8 cm, a single normal distribution function of A/m is used, whose values were derived mainly from data from the SOCIT hypervelocity impact experiments [22].

$$D(\log_{10} A/M) = N(\mu_3, \sigma_3) \quad (2)$$

Between 8 and 11 cm, a connecting function is used to bridge the two dimensional regions. The parameter values for satellite fragmentations are reported here for completeness. It can be observed that these values are defined for different (usually three) size classes; however, there is no correspondence among the parameters for these classes.

$$\alpha = \begin{cases} 0 & \lambda_c \leq -1.95 \\ 0.3 + 0.4(\lambda_c + 1.2) & -1.95 < \lambda_c < 0.55 \\ 1 & \lambda_c \geq 0.55 \end{cases} \quad (3)$$

$$\mu_1 = \begin{cases} -0.6 & \lambda_c \leq -1.1 \\ -0.6 - 0.318(\lambda_c + 1.1) & -1.1 < \lambda_c < 0 \\ -0.95 & \lambda_c \geq 0 \end{cases} \quad (4)$$

$$\sigma_1 = \begin{cases} 0.1 & \lambda_c \leq -1.3 \\ 0.1 + 0.2(\lambda_c + 1.3) & -1.3 < \lambda_c < -0.3 \\ 0.3 & \lambda_c \geq -0.3 \end{cases} \quad (5)$$

$$\mu_2 = \begin{cases} -1.2 & \lambda_c \leq -0.7 \\ -1.2 - 1.322(\lambda_c + 0.7) & -0.7 < \lambda_c < 0 \\ -2.0 & \lambda_c \geq -0.1 \end{cases} \quad (6)$$

$$\sigma_2 = \begin{cases} 0.5 & \lambda_c \leq -0.5 \\ 0.5 - (\lambda_c + 0.5) & -0.5 < \lambda_c < -0.3 \\ 0.3 & \lambda_c \geq -0.3 \end{cases} \quad (7)$$

$$\mu_3 = \begin{cases} -0.3 & \lambda_c \leq -1.75 \\ -0.3 - 1.4(\lambda_c + 1.75) & -1.75 < \lambda_c < -1.25 \\ -1 & \lambda_c \geq -1.25 \end{cases} \quad (8)$$

$$\sigma_3 = \begin{cases} 0.2 & \lambda_c \leq -3.5 \\ 0.2 + 0.1333(\lambda_c + 3.5) & \lambda_c > -3.5 \end{cases} \quad (9)$$

Despite representing the state of the art, this model presents a series of limitations, generally recognized and reported in literature.

1. Limited data for small objects (<8 cm):
   A/m distributions for the small fragments are based only on data from the SOCIT laboratory tests [25][26]. These tests provided valuable information but are limited in number and models tested; indeed, the NASA SBM does not seem to be representative of further tests performed with satellite mock-ups (e.g., Hanada's tests [20]). Direct data from fragmentation events in space are very scarce at these small sizes. The Haystack radar has provided some measurements, but with large uncertainties below 1 cm [27]. Optical sensors such as those on NASA

satellites P78-1 and P91-1 have only characterized fragments >1 cm [28]. The lack of robust observational data makes it difficult to validate A/m distributions for small debris.

2. Lack of distinction between explosions and collisions:
   The model only partially differentiate A/m distributions between explosion and collision fragments, despite the fragmentation mechanisms being different. Introducing separate distributions could improve the distributions accuracy.
3. Projection and rotation effects:
   The calculation of A/m is based on the analysis of orbital decay of catalogued debris. This approach does not take into account the effects of area projection [29] and fragment rotation [30], which can influence the decay rate [31].
4. Shape and density of fragments:
   The model assumes a simplified relationship between area and characteristic length. Irregular shapes and variable densities of fragments might require more complex relationships [32][33].
5. Updated data:
   The introduction of novel materials and design solutions in modern spacecraft are currently affecting the reliability of this model, which may require a future update.

Despite the previously discussed limitations of the NASA SBM, it is worthwhile to evaluate the characteristics of A/m distributions that are well represented by the model. A notable feature of the NASA SBM is its use of a sum of normal distributions, weighted by the coefficient α. Following tests carried out on satellite mock-ups [20], Hanada further analysed the issues related to measuring fragment cross-sections, refining an A/m model based on experimental data [21]. The model maintains a double normal distribution approach for λ_c between -2.71 and -1.01 (corresponding to 1.9 mm and 97.7 mm), with the values of α, mean, and standard deviation consistently dependent on λ_c. Specifically, Hanada classifies the two normal distributions as contributions from low and high-density materials. For characteristic lengths outside this range, it is recommended to use only the high-density distribution. The parameter values for the curves are reported below (with a correction to the formulation of α, relative to that reported in the source paper, to obtain the expected trend):

$$D(\log_{10} A/M) = \alpha \cdot N(\mu_H, \sigma_H) + (1-\alpha) \cdot N(\mu_L, \sigma_L) \quad (10)$$

$$\alpha = 1 + 0.888(\lambda_c + 2.71)(\lambda_c + 1.01) \quad (11)$$

$$\mu_H = -0.7 - 0.218\lambda_c \quad (12)$$

$$\sigma_H = 0.685 + 0.218\lambda_c \quad (13)$$

$$\mu_L = 0.554 + 0.105\lambda_c \quad (14)$$

$$\sigma_L = 0.106 + 0.0149\lambda_c \quad (15)$$

It can be clearly noted that the low-density fragments (indicated with the subscript L) present a higher mean (higher A/m values) and a reduced standard deviation (narrower "bell" curve) compared to the high-density fragments. It is important to emphasize that the main limitation of this study may be related to the lack of development of a more advanced model for larger fragments (above 0.1 m), simulated by the high-density distribution alone. This limitation is due to the fact that the studied mock-ups lacked easily detachable internal components, but mainly consisted of CFRP plates and panels connected by metal bars and spacers; this configuration deprived the object of the possibility of detachment of internal components or subsystems, which are therefore not considered in the model.

3 A/M DISTRIBUTIONS FROM GROUND AND ORBITAL DATA

In this section the comparison of the previous models with experimental and orbital data are presented. It shall be underlined that the Hanada model was not developed to be extrapolated to other cases; however, for sake of completeness, it is interesting to compare it with real data.

The experimental and orbital data employed in this analysis is listed in Table 1. The majority of the data is related to impact tests performed on ground; in addition, the COSMOS-IRIDIUM observation data is also included. This dataset is limited to just 10 cases due to the lack of complete information in literature and online databases; in particular, both A/m and Lc distributions are needed to obtain the full set of curves and distributions reported in Figure 1. In addition, to fit the whole curves in the graphs and obtain a visual comparison of the distribution shapes with the real data (red histograms), in some cases reported in the legends the NASA SBM (black solid line) and the Hanada model (blue dashed line) were scaled up (in case of “large” bell-shaped curves, that would present a smaller peak) or down (“thin” curves, with higher peaks).

Qualitatively, results show that the NASA SBM is capable to represent adequately only a few cases, with good results for test PICOSAT-01 and for the COSMOS 2251 fragmentation; it is interesting that the PICOSAT-02 and the IRIDIUM 33 cases, both representing glancing impacts, present a clear translation of the A/m distributions to larger values. It is important to underline that the COMSOS 2251 was an old satellite, compatible with the original data on which the model itself was developed.

Table 1: Ground and space data with available Lc and A/m distributions

N.	Target	REF	Experiment / observation	EMR, J/g	Central/glancing
01	HANADA–HVI	[13]	experiment	52	central
02	HANADA–LVI	[13]	experiment	61	central
03	LAN–01	[14]	experiment	71	central
04	LAN–02	[14]	experiment	55	central
05	LAN–03	[14]	experiment	48	central
06	PICOSAT–01	Internal data	experiment	78	central
07	PICOSAT–02	Internal data	experiment	78	glancing
08	CNES	[12]	experiment	19	central
09	COSMOS 2251	[11]	observation	41564	central
10	IRIDIUM 33	[11]	observation	108906	glancing

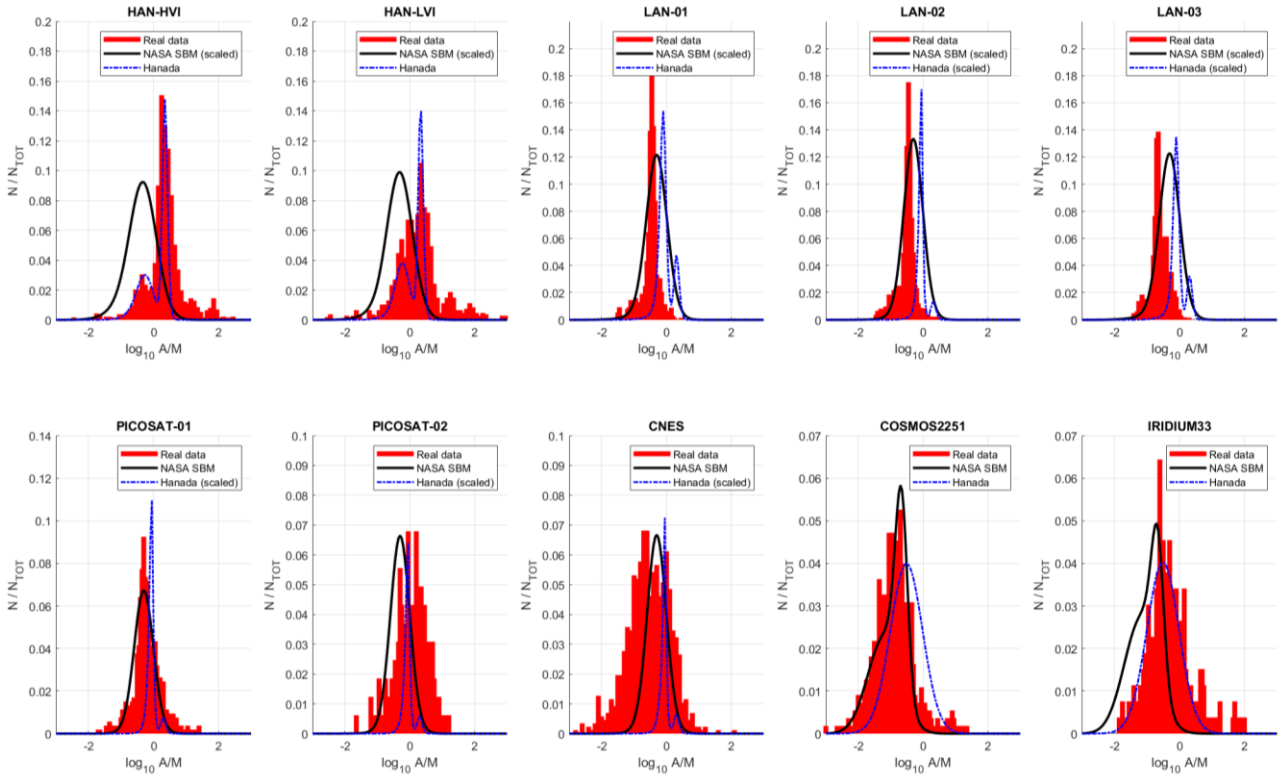

Figure 1: comparison of observed A/m data distributions with NASA SBM and Hanada model

On the contrary, the Hanada model is fitting not only the two experiments that led to its definition, but is also capable of representing the IRIDIUM-33 distribution. Its reliability with all the other ground experiments is quite low; it shall be mentioned that these experiments focused on small targets, for which model extrapolation was not initially intended.

These plots suggest that the present formulations cannot reliably represent real fragmentation data, both in terms of mode (i.e. the distribution peak position) and dispersion (i.e. the distribution width). In particular, it seems that different parameters may affect the distributions. Among them, it seems that glancing impacts (PICOSAT-02 and IRIDIUM-33) may produce fragments with larger A/m ratios; in addition, literature data also strongly suggest that the presence of low-density materials (composites, electronic components) may be produce secondary peaks at larger A/m values.

3.1 Experimental data and the relation with breakup mechanisms

A notable feature among the main characteristics of both the NASA SBM and Hanada's model is how all formulas exhibit a dependence on the characteristic length and, more generally, a typical division into three distinct sections. This feature is of particular importance, as the different fragmentation mechanisms present in an orbital break-up have already been extensively discussed, and

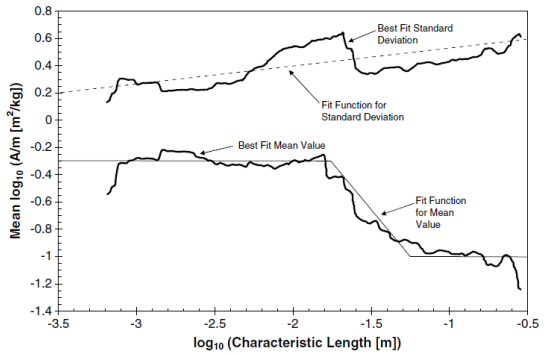

Figure 2: μ and σ trends for A/m distributions for SOCIT data (picture from [22])

their dependence on the size of the object has been noted. In particular, from the data of the SOCIT experiment [22], it can be observed that the A/m distribution can be divided into three sections, as the mean parameter varies as a function of the characteristic length (see Figure 1): a first branch with constant mean up to $\lambda_c = -1.75$ (0.017 m), a section where μ decreases linearly up to $\lambda_c = -1.35$ (0.056 m), and finally again a section with constant mean.

It is interesting to note that for the most recent characteristic length distribution model, developed in the context of this research activity and available in literature [24], the identified threshold values for the transition between the three sections would be $0.1276 \cdot L_C$ and $0.0085 \cdot L_C$, respectively. Considering a characteristic length of 0.4 m for SOCIT, these return 0.0513 m ($\lambda_c = -1.29$) and 0.0034 m ($\lambda_c = -2.47$) respectively. If SOCIT were instead considered as a "small satellite" due to its construction characteristics, the lower threshold would be calculated as $0.0405 \cdot L_C$, leading to a value of 0.0163 m ($\lambda_c = -1.79$). It shall be noted how, in this latter case, the two thresholds are practically identical to those identified by Krisko (respectively: -1.79 and -1.75, -1.29 and -1.35). This additional result suggests that the identification of the three main fragmentation mechanisms is valid and that it can be also recognized in the A/m distributions.

A further analysis of the data from the PICOSAT experiments [15][34] reveals that the dimensional classes can be also partially recognized in these dataset, despite the different geometries and materials involved in the mock-ups. Figure 3 illustrates the experimental trends of the A/m mean (blue solid line) and standard deviation (orange dashed line) for the two tests. It also shows the threshold values for the three regimes (black dashed lines) and the fragments counts for each characteristic length class (red, green, and blue histograms). For PICOSAT-01, the small-size debris (red classes) exhibit relatively high A/m ratios on average. In contrast, the intermediate range (green) shows nearly constant values, approximately -0.2 for smaller classes, which decrease to around -0.4 for larger sizes. In the third section, representing the largest satellite parts, the trend starts at about -0.2 and further decreases for the largest objects. It

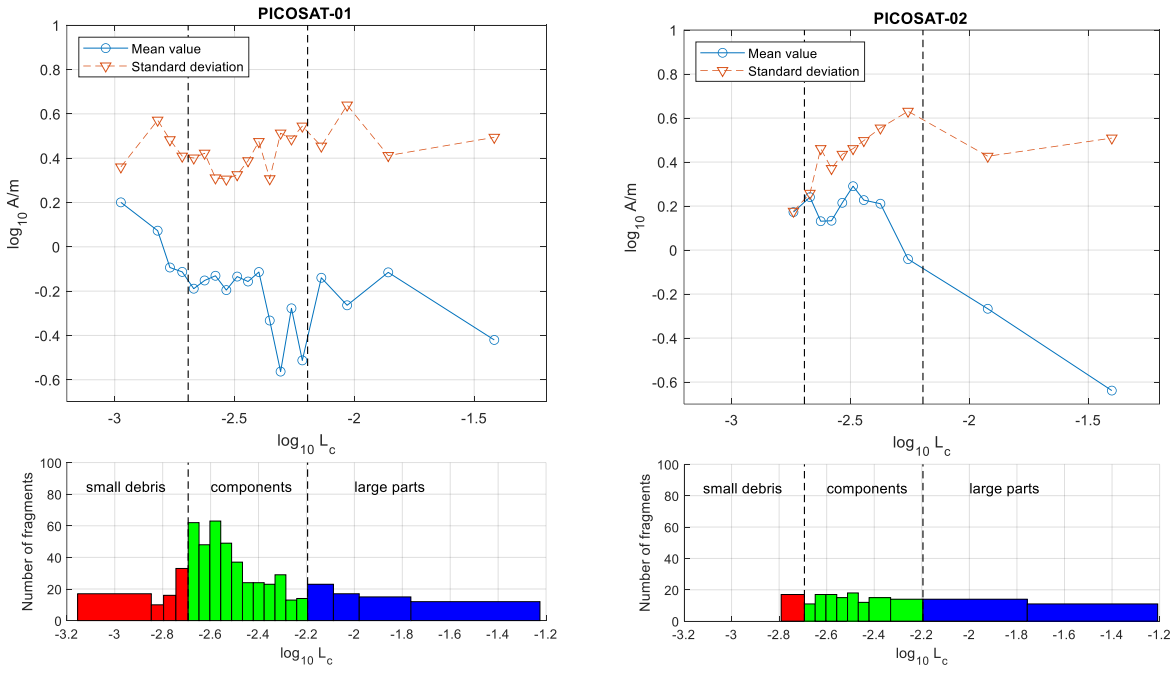

Figure 3: μ and σ trends for A/m distributions for the two PICOSAT experiments. For both cases, the number of fragments collected in each class is reported on the bottom

is noteworthy that the number of objects in the first and third sections constitutes a small fraction of the total fragment count. This trend is even more pronounced in the PICOSAT-02 data, where only a few objects are present in the first and third sections. This test involved a glancing impact, which appears to significantly influence the fragment distribution. Specifically, the central section (green) shows higher A/m average values (around 0.2). However, a reduction at larger characteristic lengths, similar to the trend observed in PICOSAT-01, is also apparent. Finally, the few large objects (blue) display a further decrease in the A/m average values.

3.2 Data analysis conclusions

The presented data revealed the limitations of current A/m distribution models. To address these shortcomings, a more representative A/m model should incorporate the following features. First, it should use sums of normal distributions, as they seems to be representative of both historical data and more recent experiments. Second, it should employ a three-section formulation, which identifies the different break-up mechanisms that affect an in-space fragmentation and the consequent debris generation. Third, it shall consider the effect of different materials and of impact conditions, such as glancing impacts.

4 CONSIDERATIONS ON A/M DISTRIBUTIONS REPRESENTATION

To date, A/m distributions are cumulatively represented as a single graph (or histogram, in case of using data from observations or experiments or synthetically generated). From a statistical point of view, the NASA SBM curve represents a cumulative PDF (Probability Density Function) (sum of PDFs in the various characteristic length classes): the integral of the curve must be equal to 1. Comparison with discrete data (such as histograms) can be complicated, as the sampling usually used is not dense enough and there may be discontinuities in the data itself; to reduce this problem, it is therefore advisable to compare the data with the model using CDFs (Cumulative Density Functions), for which such problems are mitigated. For example, Figure 4 shows the CDFs for the distributions related to the debris clouds generated by COSMOS 2251 and IRIDIUM 33; compared to the graphs in Figure 1, it is much clearer to identify the deviation of the observed data of IRIDIUM 33 from the NASA SBM curve. Moreover, for COSMOS 2251, it is also possible to better quantify the deviation between observational data and the model in the interval between -0.5 and 1. This representation is particularly useful in the case of studying distributions with a reduced number of data (less than a hundred elements), for which the classic distribution in the form of PDF becomes too subject to the presence of peaks and data concentrations. For this reason, while the representation as PDF should remain present for historical use and quick accessibility to information, it should be correlated by the presence of the CDF representation.

Another limitation of the current model is directly related to the representation of debris populations generated by different fragmentation mechanisms. To date, A/m distributions are represented cumulatively, i.e., as the sum of all curves obtained for different characteristic length classes. Tis representation can lead to the loss of relevant information about debris populations, as large objects (which are of great interest) may constitute only a fraction compared to smaller fragments. For example, in the "PICOSAT" tests carried out at CISAS [15][34], the characteristic length model identified 68 and 386 fragments for PICOSAT-01, and 26 and 119 fragments for PICOSAT-02, in classes (1) and (2) respectively. Class (1) represents large parts, while class (2) represents detached components. With these numbers, it's clear that peculiar characteristics for the large-size population could be lost, as their weight in the general representation becomes negligible. This can happen even more when small debris (class 3) are included: where measured, they can reach numbers orders of magnitude higher than fragments in larger size classes. Finally, there is the problem of data truncation: both for observations and experiments, there is a maximum resolution, depending on the instrumentation used and, for observations, on the orbit in which the fragmentation occurred. This limit can significantly modify the A/m distributions, as setting a minimum limit to the characteristic length falls into one of the previously introduced classes with all the problems described above. At the same time, not setting such a limit may lead to the inclusion of data in the A/m distributions that are not compatible with the observed population.

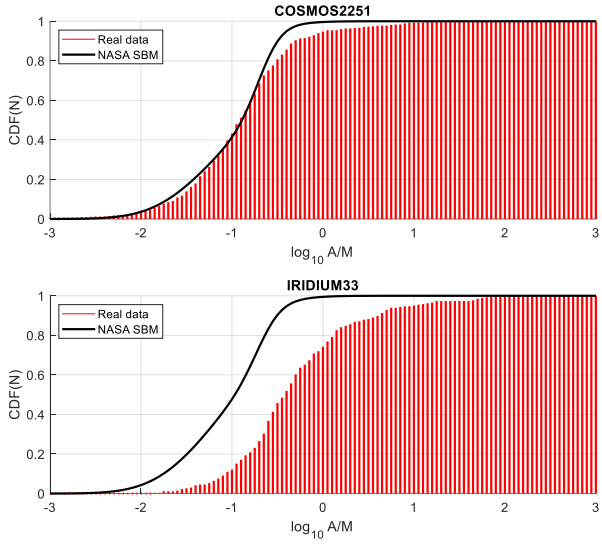

Figure 4: CDFs of A/m distributions for debris from COSMOS 2251 and IRIDIUM33

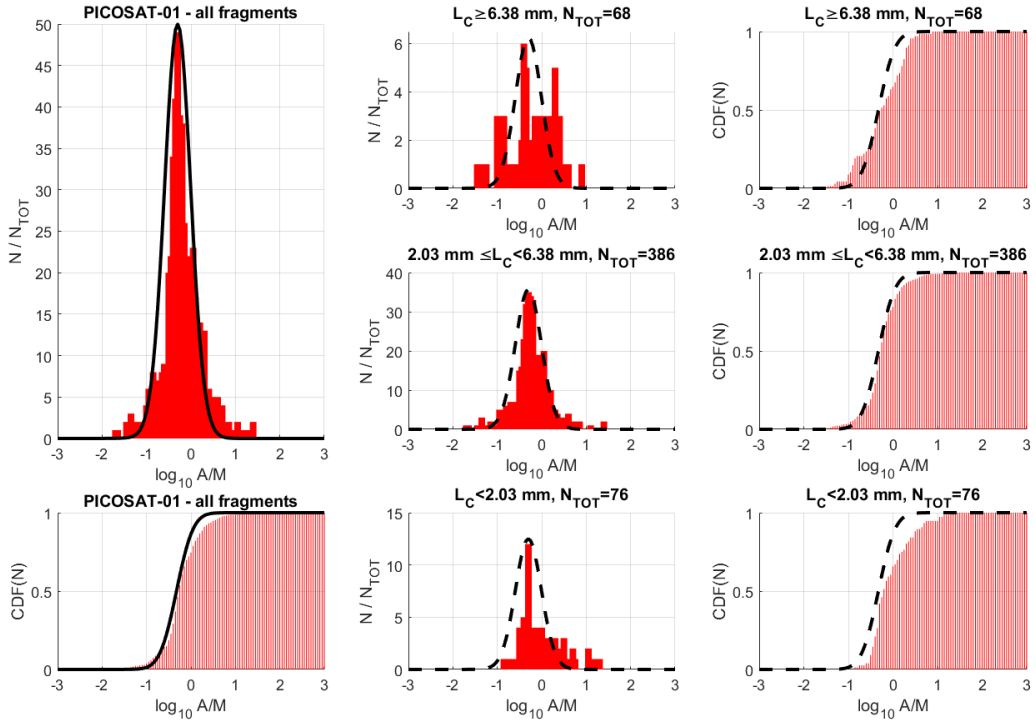

Figure 5: A/m distribution and related CDF for the PICOSATELLITE-01 test: on the left, the cumulative data; on the right, the division by size classes identified by the characteristic length model. In black, the NASA SBM model; in red, the experimental data.

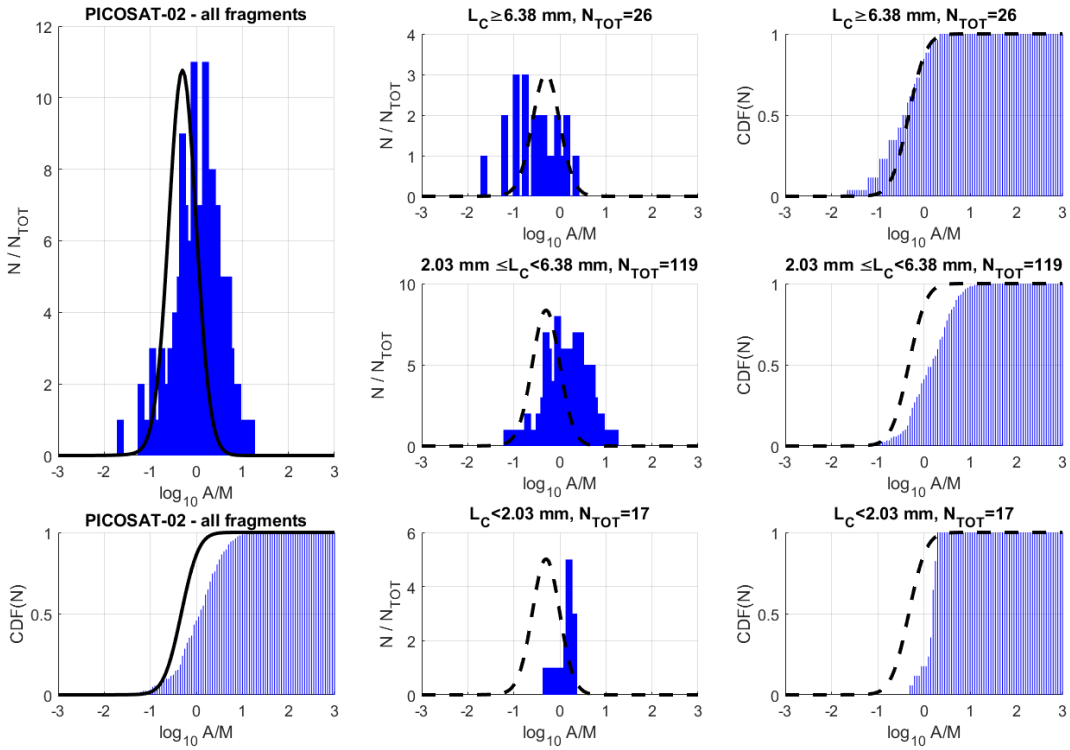

Figure 6: A/m distribution and related CDF for the PICOSATELLITE-02 test: on the left, the cumulative data; on the right, the division by size classes identified by the characteristic length model. In black, the NASA SBM model; in blue, the experimental data.

In Figure 5 and Figure 6, the experimental A/m distributions from the tests performed at CISAS on the PICOSAT mock-ups are represented. In the first case, defined as a central impact, it can be observed that the NASA SBM model is fairly representative of the central population, while for larger fragments it loses a fraction of the population between -1 and 0.5 and underestimates the number of objects between -0.5 and 0.5; for smaller fragments, reduced in number due to resolution limits reached, the NASA SBM curve instead shows a substantial error although it is able to precisely identify the central peak. For the PICOSAT-02 case, the problem is even more visible, with the NASA SBM curve shifted to lower A/m values for medium and small-sized fragments.

In conclusion, the need to maintain the representation divided into three different sections, defined by the size classes of the fragments, is emphasized. Furthermore, the usefulness of using CDFs to evaluate the quality of proposed models compared to experimental, observational, or synthetic data is highlighted.

5 A/M MODEL DEVELOPMENT STRATEGY

The development of a new model for A/m distributions is based on the following guidelines, drawn from the previous sections and summarized here:

1. The model must be represented by sums of normal distributions.
2. The model must be divided into three sections, representing the size classes defined in the new proposed characteristic length distribution model (see [24]).
3. The curve parameters (weight, mean, standard deviation) must be a function of the characteristic length; this does not preclude them from also being a function of other impact parameters, such as the involved materials and the impact conditions (e.g. glancing versus central collisions).
4. The model's ability to represent experimental data must also be evaluated through the use of CDFs.

The main problems to be addressed in developing this model are related to the quantity and quality of available data. To date, the research group has managed to recover distributions of both characteristic length and A/m for only 10 cases; however, it should be noted that the direct association of characteristics to the individual debris (i.e., knowing that for a certain debris there is a certain value of Lc and A/m) is possible only for internal data (the two reported tests on PICOSAT), while this information is not present for other datasets. Fortunately, for both COSMOS 2251 and IRIDIUM 33, it is possible to associate the totality of fragments to class 2 alone, as no information is present on the small-size debris population (section 3), while the Lc model does not predict the survival of intact parts (section 1). Finally, the use of Hanada's data needs to be evaluated, as the representativeness of the experiments themselves is questionable, having replaced internal components with CFRP plates in the mock-ups; this modification could significantly influence the distribution of fragments in the second size class.

In the coming months, it is planned to continue developing an A/m model based on these requirements and to seek additional sources of distributions (experimental or from literature).

6 CONCLUSIONS

This paper highlighted the limitations of current area-to-mass (A/m) models and representations used in space debris analysis. It demonstrated the need for a new model that builds on the existing approach of summing normal distributions while also accounting for the geometrical and material properties of the involved bodies. Specifically, it is recommended to develop separate models for three distinct size classes, each corresponding to a different breakup mechanism observed in spacecraft collisions:

1. Large Surviving Parts – Major components that remain mostly intact after the event.
2. Detached Components – Smaller parts that break away from the main structure.
3. Fragmented Debris – Fine debris resulting from the complete fragmentation of directly impacted sections.

This approach would also allow for a separate implementation of the three regimes within fragmentation and propagation software. In this way, it would be possible to consider the real influence of each class on the debris environment, with a particular advantage for long-term propagation, which is strongly affected by A/m values.

Additionally, it is proposed to represent A/m trends using cumulative distributions. This approach would enhance model validation and comparison with real data by minimizing the occurrence of peaks and data clustering that can distort the visualization of actual distributions.

Future research will focus on acquiring new A/m distributions from both observations and experimental data. This effort aims to refine the parameters influencing A/m distributions and support the development of an improved, more accurate model.

AKNOWLEDGEMENTS

This work has been supported by the Italian Space Agency in the framework of the agreement n.2023-37-HH.0 “Attività tecnico-scientifiche di supporto a C-SSA/ISOC”.

7 REFERENCES

[1] Anz-Meador, P., Opiela, J., & Liou, J. C. (2023). *History of on-orbit satellite fragmentations* (No. NASA/TP-20220019160).

[2] Kessler, D. J., et al. (2010). The Kessler syndrome: implications to future space operations. *Advances in the Astronautical Sciences*, *137*(8), 2010.

[3] Pardini, Carmen, and Luciano Anselmo. "Evaluating the impact of space activities in low earth orbit." *Acta Astronautica* 184 (2021): 11-22.

[4] Mrusek, B., & Weiland, L. (2023, March). Space Commercialization and the Rise of Constellations: The Resulting Impact on the Kessler Effect. In *2023 IEEE Aerospace Conference* (pp. 01-07). IEEE.

[5] Olivieri, L., & Francesconi, A. (2020). Large constellations assessment and optimization in LEO space debris environment. *Advances in Space Research*, *65*(1), 351-363.

[6] Johnson, N. L., et al. (2001). NASA's new breakup model of EVOLVE 4.0. *Advances in Space Research*, *28*(9), 1377-1384.

[7] Anselmo, L., & Pardini, C. (2010). Long-term dynamical evolution of high area-to-mass ratio debris released into high earth orbits. *Acta Astronautica*, *67*(1-2), 204-216.

[8] Belkin, S. O., & Kuznetsov, E. D. (2021). Orbital flips due to solar radiation pressure for space debris in near-circular orbits. *Acta Astronautica*, *178*, 360-369.

[9] Linares, R., et al. (2012). Space object area-to-mass ratio estimation using multiple model approaches. *Advances in the Astronautical Sciences*, *144*, 55-72.

[10] Kaminski, K., et al. (2019). Low LEO optical tracking observations with small telescopes. In *Proceedings of the 1st NEO and debris detection conference, Darmstadt, Germany* (pp. 22-24).

[11] Anselmo, Luciano, and Carmen Pardini. "Analysis of the consequences in low Earth orbit of the collision between Cosmos 2251 and Iridium 33." *Proceedings of the 21st international symposium on space flight dynamics*. Vol. 294. Centre nationale d'etudes spatiales Paris France, 2009.

[12] Abdulhamid, H., et al. (2021, April). On-ground HVI on a nanosatellite. Impact test, fragments recovery and characterization, impact simulations. In *Proceedings of the 8th ESA Space Debris Conference, Darmstadt, Germany* (Vol. 20).

[13] Liou, J. C., et al. "Micro-satellite impact tests to investigate multi-layer insulation fragments." *5th European Conference on Space Debris*. No. JSC-CN-17534. 2009.

[14] Lan, Sheng-wei, et al. "Debris area distribution of spacecraft under hypervelocity impact." *Acta Astronautica* 105.1 (2014): 75-81.

[15] Olivieri, L., et al. (2022). Characterization of the fragments generated by a Picosatellite impact experiment. *International Journal of Impact Engineering*, *168*, 104313.

[16] Pardini, C., & Anselmo, L. (2014, June). Review of the uncertainty sources affecting the long-term predictions of space debris evolutionary models. In *Proceedings of the 3rd european workshop on space debris modelling and remediation, CNES Headquarters, Paris* (pp. 16-18).

[17] Muntoni, G., et al. (2021). Crowded space: a review on radar measurements for space debris monitoring and tracking. *Applied Sciences*, *11*(4), 1364.

[18] Schimmerohn, M., et al. (2021). Numerical investigation on the standard catastrophic breakup criteria. *Acta Astronautica*, *178*, 265-271.

[19] Francesconi, A., et al. (2022). Numerical simulations of hypervelocity collisions scenarios against a large satellite. *International Journal of Impact Engineering*, *162*, 104130.

[20] Hanada, Toshiya, et al. "Outcome of recent satellite impact experiments." Advances in Space Research 44.5 (2009): 558-567.

[21] Hanada, Toshiya, et al. "For better calculation of the average cross-sectional area of breakup fragments." *Transactions of the Japan Society for Aeronautical and Space Sciences, Space Technology Japan* 7.ists26 (2009): Pr_2_25-Pr_2_30.

[22] Krisko, P. H., et al. (2008). SOCIT4 collisional-breakup test data analysis: With shape and materials characterization. *Advances in Space Research*, *41*(7), 1138-1146.

[23] Olivieri, L., et al. (2023). Simulations of satellites mock-up fragmentation. *Acta Astronautica*, *206*, 233-242.

[24] Olivieri L, Francesconi A. (2025) A novel size distribution model for debris generated by in-orbit collisions. *International Journal of Impact Engineering.*

[25] McKnight, D.S., et al. "Satellite Orbital Debris Characterization Impact Test (SOCIT) Series Data Collection Report" (1995a)

[26] McKnight, D.S., et al. "Analysis of SOCIT Debris Data and Correlation to NASA's Breakup Models" (1995b)

[27] Stansbery, E.G., et al. "Haystack Radar Observations of the Orbital Debris Environment" (1994)

[28] Mulrooney, M.K., et al. "Micro-Meteoroid/Orbital Debris Environment for LDEF's Orbit" (2008)

[29] Hanada, Toshiya, and J-C. Liou. "Theoretical and empirical analysis of the average cross-sectional areas of breakup fragments." *Advances in Space Research* 47.9 (2011): 1480-1489.

[30] Mulrooney, M.K. and Matney, M.J., "Modeling Potential Cubesat Orbital Debris: A Study on CubeSat Orbital Decay and Reentry Utilizing Analytical Drag Calculations." Proceedings of the 6th European Conference on Space Debris, Darmstadt, Germany, 2013.
[31] Anselmo, L. and Pardini, C., "Orbital element estimation and prediction through atmospheric density determination from orbital data of the LARES satellite." Proceedings of the 6th European Conference on Space Debris, Darmstadt, Germany, 2013.
[32] Francillout, L.S., Anselmo, L. and Pardini, C., "Comparison of the orbital decay of spherical and boxed-shaped objects using two analytical models." Proceedings of the 6th European Conference on Space Debris, Darmstadt, Germany, 2013.
[33] Pardini, C., Anselmo, L. and Rossi, A., "Drag and energy dissipation in the orbital dynamics of objects with complex geometries." Proceedings of the International Astronautical Congress, IAC-14-A6.2.8, 2014.
[34] Lopresti, S., et al. (2023). Glancing Impact on a Picosatellte Mock-up: Test Results. In *Proceedings of the International Astronautical Congress, IAC* (Vol. 2023). International Astronautical Federation, IAF.